PAPER

Check for updates

Techno-economic and life cycle analyses of the synthesis of a platinum–strontium titanate catalyst†

Sultana Ferdous,[a] Ulises R. Gracida-Alvarez, [iD][b] Magali Ferrandon,[c] Massimiliano Delferro, [iD][c] Pahola Thathiana Benavides [iD] *[b] and Meltem Urgun-Demirtas [iD] *[a]

The heterogeneous platinum/strontium titanate (Pt/SrTiO₃ or Pt/STO) catalyst has garnered significant attention as a promising candidate for the hydrogenolysis of polyolefins to hydrocarbon oils. This study evaluates the cost and environmental impacts of a newly developed scalable Pt/STO catalyst production, which includes the synthesis of the STO support and the deposition of Pt onto the support. This two-step synthesis plays a significant role in assessing the commercial feasibility of the catalyst, while energy consumption during the process plays an important role in its environmental impacts. The CatCost and the Research and Development Greenhouse Gases, Regulated Emissions, and Energy use in Technologies (R&D GREET) models were used, respectively, to perform techno-economic analysis (TEA) and life cycle analysis (LCA) of the newly developed catalyst. The TEA showed that the raw materials, accounting for approximately 76% of the total operation cost, has a profound effect on the estimated catalyst cost, mainly due to the platinum precursor. The LCA findings indicated that the catalyst production generates greenhouse gas (GHG) emissions of 66 kg CO_2e per kg, primarily due to the use of solvents and electricity in the process. The sensitivity analysis indicated that the total operating costs (OpEX), platinum precursor cost, and spent catalyst value (SCV) significantly impact the cost of the synthesized catalyst. Additionally, adopting solvent recovery strategies and using renewable electricity can reduce the GHG emissions of catalyst production to 29 kg CO_2e per kg.

Introduction

Catalytic hydrogenolysis is a promising technology for the conversion of waste polyolefins into liquid and wax-like products using metal nanoparticle catalysts dispersed on a metal oxide support at the laboratory scale.[1–3] Atomic layer deposition (ALD) is a well-established technique for introducing platinum (Pt) nanoparticles onto strontium titanate (STO [SrTiO₃]), resulting in a Pt/STO heterogeneous catalyst that is effective for the selective hydrogenolysis of polyolefins to hydrocarbon oils.[3] However, ALD faces challenges in scaling up production beyond the gram scale

within a short timeframe, primarily due to the requirement of highly specialized instrumentation.[3] Due to the expensive and support-intensive ALD method used during synthesis, it is crucial to adeptly scale up catalyst production and accelerate the upcycling processes.[3] Consequently, a new procedure has been developed for scaling up the production of Pt/STO and expediting the commercialization of hydrogenolysis processes.[3] Surface organometallic chemistry (SOMC) is an analogous technique to ALD that can be used to synthesize hydrogenolysis catalysts like Pt/STO. SOMC is scalable and an appropriate target for large-scale catalyst deposition.[3,4] To optimize catalyst activity and selectivity for processes as widespread as metathesis, polymerization, hydrogenation, and hydrogenolysis, SOMC-derived well-maintained catalysts have been modified through precursor engineering and support control in the last forty years.[3,4]

Pt/STO was found to be more effective in converting polyolefin waste to narrowly distributed liquid alkane products for lubricants than other Pt-based catalysts.[1,5] Pt catalysts supported on silica, Pt/SiO₂–Al₂O₃, and Pt/STO have the highest yield of liquid/wax products. However, Pt/STO produces non-branched liquids. This is attributed to the high

[a] *Applied Materials Division, Argonne National Laboratory, 9700 S Cass Ave, Lemont, IL, 60439, USA. E-mail: demirtasmu@anl.gov*
[b] *LCA and Technology Assessment Department, Energy Systems and Infrastructure Assessment Division, Argonne National Laboratory, 9700 S Cass Ave, Lemont, 60439, USA. E-mail: pbenavides@anl.gov*
[c] *Chemical Sciences and Engineering Division, Argonne National Laboratory, 9700 S Cass Ave, Lemont, IL, 60439, USA*
† Electronic supplementary information (ESI) available: Additional experimental and analysis details, materials, and methods, as well as additional results. See DOI: https://doi.org/10.1039/d5cy00189g

This journal is © The Royal Society of Chemistry 2025

Catal. Sci. Technol., 2025, **15**, 4419–4429 | **4419**

stability of Pt on STO support. Importantly, the liquid product could be used as a drop-in base oil in tribological applications. However, Pt/SiO$_2$–Al$_2$O$_3$ comprises alkyl-aromatics, and the presence of alkyl-aromatics in base oil could have a negative impact on the tribological properties (*e.g.*, friction and wear). This makes the liquid product obtained by the hydrogenolysis of plastic waste catalyzed by Pt/STO highly desirable. Because of the high dispersion, small particle sizes (<2 nm) and high stability of Pt supported on STO, Pt/STO could be advantageous in applications such as hydrogen production, water-splitting photocatalysis, and waste plastic conversion.[2,6,7]

Few sources are accessible for researchers outside the well-known catalyst manufacturing companies to estimate the cost of the materials associated with catalyst production, especially at the industrial scale.[8] Commercialization of the catalysts is a complex and unspecified process. The production cost of the catalytic material may vary significantly between the industrial and laboratory scales.[8] Due to the limited availability of tools to evaluate the catalyst cost *via* techno-economic analysis (TEA), the cost of catalyst manufacturing is often ignored in the initial stages.[9] Similarly, catalysts are often overlooked in biofuel life-cycle analysis (LCA) due to a lack of understanding and publicly available information about catalyst production, which is often proprietary.[10] Recent publications and reports claimed that catalyst cost contributes between 3 and 9% of the total installed equipment cost for biomass conversion processes involving catalytic fast pyrolysis and indirect liquefaction.[8] This could bring a ±10% change in the minimum fuel selling price depending on the catalyst cost.[8–12] In other processes, such as the production of hydrocarbon fuels from lignocellulose biomass *via in situ* and *ex situ* fast pyrolysis, the catalyst cost can comprise up to 24% of the total operating cost.[13–15] A recent study on catalytic fast pyrolysis of mixed plastic waste shows that the minimum selling price of a benzene, toluene, and xylene (BTX) mixture increases by 16% from the base case with the rise of the catalyst cost from $2.98 per kg to $6.75 per kg.[16] In terms of LCA, it has been found that catalysts can affect the greenhouse gas (GHG) emissions of biofuel production. For instance, Benavides *et al.* found that catalysts' influence on the life-cycle GHG emissions of biofuels was dictated by the GHG intensity of producing catalysts and their consumption rates.[10] Also, according to the International Energy Agency, progress in catalysts and related processes could potentially lower the energy strength of the most carbon-intensive chemical products by 20 to 40%.[17]

As a result, catalysis research should target the reduction of economic and environmental impacts by increasing resource efficiency.[9] To fulfill this goal, the newly manufactured catalysts should be assessed against a standard that includes catalytic activity, selectivity, availability of chemicals, and conversion productivity along with the cost and environmental impacts accompanying their applications.[9,13,15] It is necessary to constantly assess

the new catalyst materials with the greatest chance of success since the route from the manufacturer to the marketplace is long and costly.[9] Though hardly discussed in the literature, there is growing interest in the economic and environmental assessments of the synthesis of new catalysts among researchers who certainly understand the significance of the catalyst cost and environmental impact.[9]

Because catalyst costs are likely to have an important effect on the overall cost of the production of lubricant oils from upcycled plastics,[18] this work discusses the scaled-up manufacturing, TEA, and LCA of a scalable method for the Pt/STO catalyst made by SOMC using the Pt precursor trimethyl(methylcyclopentadienyl)platinum(IV). Additionally, single-point sensitivity analyses are carried out on several key input TEA parameters, including OpEX, Pt precursor cost, total raw material cost, total capital costs (CapEX), spent catalyst value (SCV), plant size, labor cost, plant life, and selling margin, to investigate their relative significance and influence on the process and economic uncertainties involved in assessing the production cost of Pt/STO. Similarly, the effect of material recycling (*i.e.*, solvent recovery) and sources of electricity on the GHG emissions of the Pt/STO catalyst were evaluated through sensitivity analyses. These sensitivity analyses enable researchers to pinpoint the materials, market factors, and processing steps that provide the greatest potential for further process improvement.[9]

Materials and methods

This section describes the catalyst synthesis at the laboratory scale followed by its scaled-up manufacturing. The inventory data used for the TEA and LCA are constructed based on the synthesis scale used in the laboratory. Details of the TEA and LCA along with the sensitivity cases are also described.

Synthesis of Pt/STO at laboratory scale

As described by previous literature,[2,3] the catalyst synthesis was carried out in three steps: (1) synthesis of STO nanocuboids, (2) treatments of STO nanocuboids, and (3) deposition of Pt onto STO nanocuboids. This section briefly summarizes the entire synthesis procedure described in the literature mentioned above.

For the STO nanocuboid synthesis, 38.7 g of strontium hydroxide octahydrate (Sr(OH)$_2$·8H$_2$O) were added to a solution of 48.0 g of acetic acid (CH$_3$COOH) and 640.0 g of water (H$_2$O) and stirred for 2 h. Separately, 27.6 g of titanium tetrachloride (TiCl$_4$) was dissolved in 505.0 g of ethanol (C$_2$H$_6$O) and stirred for 10 min. Then, both solutions were mixed and stirred for an additional 10 min in a 2000 mL Erlenmeyer flask. A solution of 276.9 g of 10 M NaOH was injected into the previously mixed solutions for 28 min at a flow rate of 10 mL min^{-1} using a syringe pump. After simultaneously mixing and stirring, the final solution was allowed to sit for 10 min, with sedimentation occurring at a

pH of 13.0. Afterward, the solution with the sediment was transported to a reactor (4 L Hastelloy C-276) with an internal impeller and a heating jacket. For the next 2 h, the reactor was heated to 240 °C at a rate of 2 °C min^{-1} with a stir speed of 400 rpm. After completing the hydrothermal reaction, the reactor was allowed to cool at a constant rate of 2 °C min^{-1}. The solution pH was 13.2, and the products (liquid and precipitate) were placed in a new container. After washing the precipitate under vacuum filtration, it was dried in air for 12 h at 110 °C (overnight).

The synthesized STO nanocuboids were calcined in a muffle furnace at 550 °C for 4 h. The STO powder was then heated up to 200 °C under vacuum, followed by a treatment of 8% ozone in oxygen (O$_2$) at a flow rate of 400 standard cubic centimeters (sccm) by using an ozonolyzer (Pacific Ozone, Evoqua Water Technologies LLC) for 2 h. The STO powder was then subjected to nitrogen (N$_2$) bubbling through water at ambient temperature, still at 200 °C for another 2 h. For the deposition of Pt onto STO, the metalation step was carried out in an N$_2$-filled glovebox (less than 0.1 ppm H$_2$O and O$_2$). First, a solution of trimethyl(methylcyclopentadienyl)platinum(IV) (MeCpPtMe$_3$) (Sigma Aldrich, 98%) in dodecane (target 1 wt% Pt) was prepared. Then, STO powder (200 °C, 12 h) was added to the solution and the suspension was heated up to 120 °C. After 72 h, the suspension was allowed to cool down to room temperature and the metalated powder was washed and filtered three times with toluene, to remove the physisorbed precursor, and one last time with pentane, for solvent exchange. The powder was then taken out of the glove box and vacuum-dried at 60 °C overnight. Finally, the sample powder was reduced under 10% hydrogen at 300 °C for 4 h.

Scaled-up production analysis

Fig. 1 shows a block diagram of the different stages involved in the process, which also served as a guide for establishing material, energy, and equipment requirements. A modular catalytic reactor was designed for the single-use polyolefin conversion to lubricating oils from upcycled plastics. The transformation of polyolefin waste into valuable lubricants could promote a circular economy for plastics and reduce the environmental impacts of plastics' end-of-life. The process was conducted through the hydrogenolysis of upcycled waste in a reactor containing the feedstock along with the Pt/STO catalyst.[19] The scaled-up Pt/STO catalyst production was designed for a plant capacity of 25 MT per year. This estimate assumes that the catalyst will be used in a feedstock-to-catalyst ratio of 1:10 for a hydrogenolysis process for converting 250 MT of plastic film to high-quality base oils. The catalyst is manufactured in batches of approximately 285 kg, with each batch requiring 90 h. This results in a catalyst production rate of 3.2 kg h^{-1}. The equipment quantities and sizes required for producing each batch of the catalyst are detailed in Table S1 of the ESI.† These data were utilized to estimate the CapEx for the catalyst production. An important component of the analysis was the estimation of the material and energy requirements of the process. The material requirements were estimated based on the quantities established by the experimental procedure. The materials needed for producing the support (STO) were adjusted to reflect the quantities needed for catalyst production, given that the catalyst consists of 99% support and 1% Pt. Tables S2 and S3 in the ESI† present the aggregated material requirements normalized for producing 1 kg of catalyst.
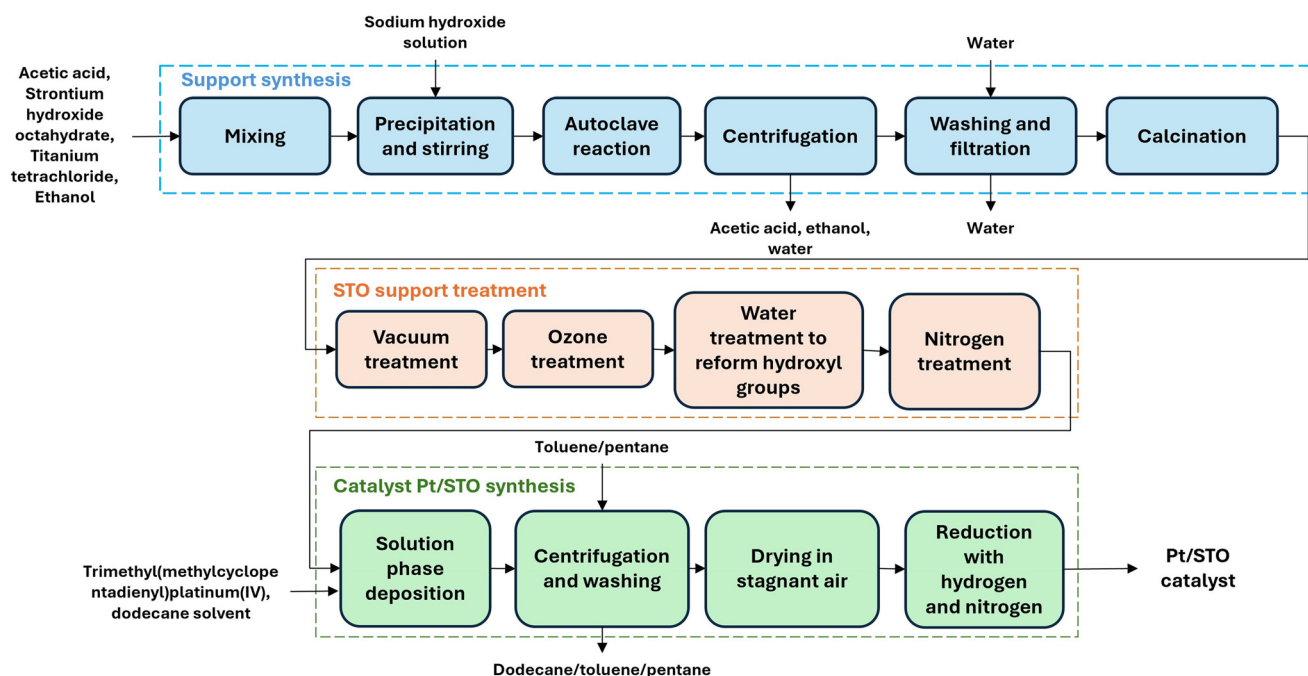

Fig. 1 System boundary used to conduct the TEA and the LCA of the synthesis of the Pt/STO catalyst.

This journal is © The Royal Society of Chemistry 2025

Catal. Sci. Technol., 2025, **15**, 4419–4429 | **4421**

The estimation of the energy requirements at different stages depended on the equipment used. For the autoclave and solution phase deposition reactors, energy calculations followed the methodology described by Majeau-Bettez et al.[20] and Kingsbury and Benavides.[21] Their estimates included the energy needed to heat reactants and solvents (Q_{react}), compensate for heat losses from the reactor surface (Q_{loss}), and power for stirring the reactor contents (Q_{stir}). The calculation of Q_{react} was based on the reaction temperature, the heat capacity of the reactants and solvents, and the amounts of reactants and solvents utilized per unit of product. To account for the effects of heat integration within the process, only half of the energy estimated in Q_{react} was incorporated into the total energy estimations of the reactor.[20] The magnitude of Q_{loss} was determined by the reactor volume and the reaction time, while Q_{stir} was obtained by multiplying a power consumption rate of 2.1 kJ h^{-1} L^{-1} by the reaction time.[20]

The electricity required for centrifugation was established as 4.4 kJ L^{-1} according to specifications from industrial equipment.[22] The energy required for the muffle furnace was obtained from vendor specifications, which indicated a power requirement of 64.8 MJ h^{-1} to reach a maximum temperature of 1200 °C. The energy required for various stages using the muffle furnace, such as calcination, treatment with ozone, hydroxyl groups reforming with nitrogen, drying in stagnant air, and reduction with hydrogen and nitrogen, was estimated according to Tschernitz et al.[23] This estimation involved multiplying the power needed to achieve the maximum temperature (64.8 MJ h^{-1}) by the division of the operation temperature of the stage over the maximum

temperature (1200 °C) raised to the third power, and then by the operation time of the furnace for that stage. The energy requirement for the vacuum oven was estimated from manufacturer specifications,[24,25] which indicated that achieving a maximum operating temperature of 220 °C required a power of 3.8 MJ h^{-1}. Additionally, the energy needed for ozone generation was also provided by a vendor, accounting for 90 MJ kg^{-1} of ozone.[26] The energy consumption for the process normalized to produce one kg of catalyst is shown in Table S4 of the ESI.†

Techno-economic analysis (TEA)

The production cost of Pt/STO was estimated with CatCost, a catalyst cost estimation model, that allows fast and up-to-date cost-based results in the research and commercialization of catalysts, which was developed by the Department of Energy (DOE) Chemical Catalysis for Bioenergy (ChemCatBio) consortium.[27] The net production cost of the synthesized Pt/STO was estimated by incorporating CapEX, OpEX, SCV, and the selling margin. The different cost components included in the TEA of the Pt/STO catalyst are shown in Fig. 2.

The detailed equipment list with the prices obtained from the vendors and other resources is presented in Table S1 of the ESI.† Raw material prices and utility costs were assessed through a combination of vendors and available price databases, provided in Table S5 of the ESI.† All raw material and chemical prices were adjusted to the year 2023 USD by the Producer Price Index for industrial chemicals[28] and, for equipment costs, the Chemical Engineering Plant Cost Index.[29] All the CapEX and OpEX assumptions used to assess
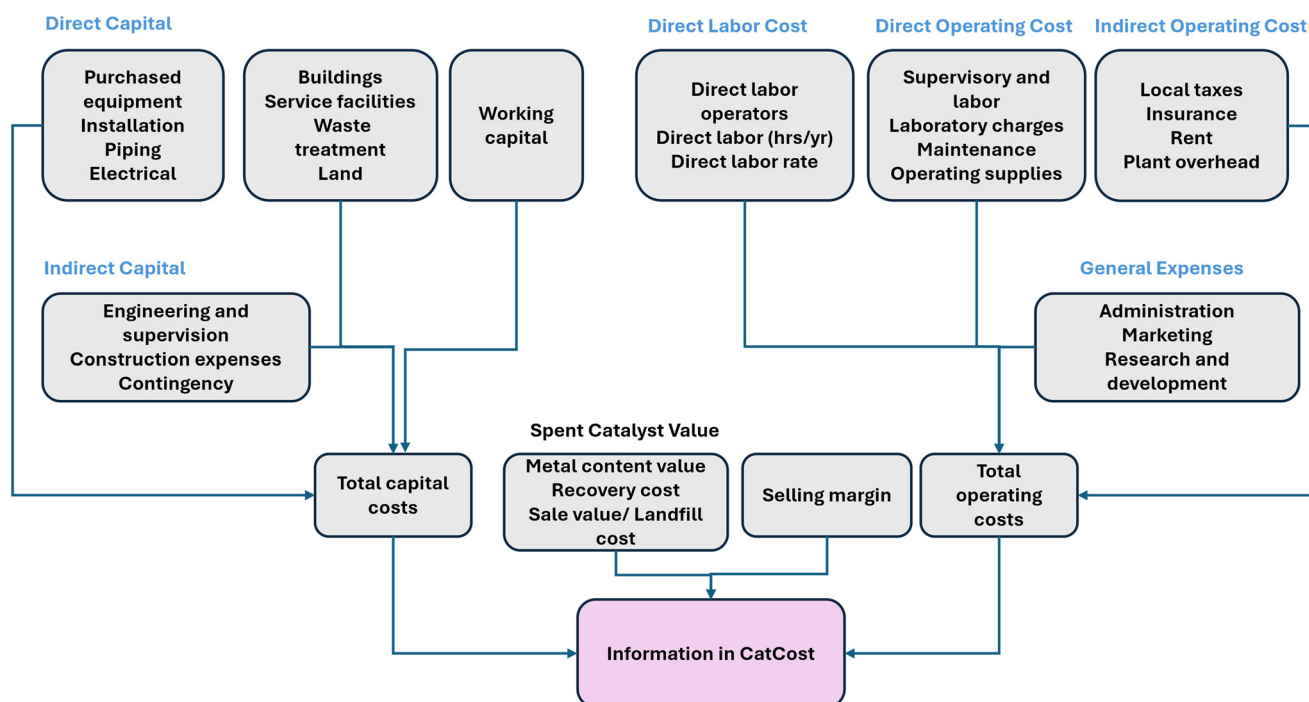

Fig. 2 Estimation of the Pt/STO catalyst cost including the cost components in the CatCost.

4422 | Catal. Sci. Technol., 2025, 15, 4419–4429

This journal is © The Royal Society of Chemistry 2025

the catalyst cost, including cost items and cost factors are provided in Tables S6 and S7 of the ESI.† The SCV was estimated considering the 8% losses incurred during the Pt recovery (see Table S8 in the ESI†).

The catalyst plant was designed for an annual production of 25 MT with 7884 h of operation per year (including maintenance and downtime). The plant is projected to have a lifespan of 20 years. The assumed return on capital invested pre-tax (selling margin) is 25% per year. The labor rate, including benefits, for year-round operating hours with full staffing during maintenance and downtime, was assumed to be $48 per h.[27] In a commercial manufacturing setting, a slightly higher quantity of materials needs to be purchased than the required amount to account for the expected losses during processing. Therefore, a factor of 3% was considered for the raw material costs to incorporate the waste and spoilage during material handling in the process.[27]

Life-cycle analysis

The goal of the LCA was to estimate the GHG emissions associated with the production of the catalyst. To conduct the LCA, material and energy requirements (life cycle inventory) for the process were analyzed using the Research and Development Greenhouse Gases, Regulated Emissions, and Energy Use in Technologies model version 2023 (R&D GREET 2023).[30] R&D GREET calculates GHG emissions based on the 100-year global warming potential values from the Intergovernmental Panel on Climate Change's (IPCC) sixth Assessment Report, which are 1.0 for carbon dioxide (CO_2), 29.8 for methane (CH_4), and 273 for nitrous oxide (N_2O).[31] The scope of the LCA was cradle-to-gate, comprising all the stages shown in Fig. 1.

The results were reported on a functional unit of one kg of catalyst produced. Allocation methods were not applied because the by-products obtained from the process were discarded as residues. Life cycle inventory data of the materials used in the production process were sourced from R&D GREET 2023 (ref. 30) and other literature studies.[32–37] The GHG emissions of general Pt production were utilized as a proxy due to missing information on the environmental impacts of trimethyl(methylcyclopentadienyl)platinum(IV). Heating requirements were met using steam produced from natural gas at a thermal efficiency of 85%, while the power requirements of the process were supplied by the U.S. average grid electricity.[30]

Given the considerable amount of solvent discarded during the process, a sensitivity analysis was conducted to explore the impact of solvent recovery in the GHG emissions of catalyst production. This analysis considered the recovery of ethanol, pentane, toluene, and dodecane, with recycling rates of 25, 50, and 75%. All discarded solvents are obtained after centrifugation (see Fig. 1). For toluene, pentane, and dodecane, it was assumed that up to 75% recycling would not require additional processing beyond pumping, whose associated energy was considered negligible. In contrast,

ethanol, which is obtained as a mixture with water and acetic acid after centrifugation, requires separation, for which additional energy is required. This mixture consists of 75 wt% water, 21 wt% ethanol, and 4 wt% acetic acid. A heuristic rule suggesting that separation through conventional distillation constitutes 40% of the energy requirements of a process was used to approximate the energy required for separation.[38] This rule was adapted for this scenario analysis by assuming that solvent recycling rates of 25, 50, and 75% would account for 10, 20, and 30% of the energy used through the stages of mixing, autoclave reaction, and centrifugation of the support production, respectively. Based on these assumptions, the additional energy consumption for the separation of ethanol is estimated at 3.7, 8.2, and 14.1 MJ kg^{-1} catalyst for the recycling rates of 25, 50, and 75%, respectively.

Since most of the equipment used for the production process is powered by electricity, an additional sensitivity analysis considered the effects of using different electricity sources on the GHG emissions of the catalyst. In this analysis, the GHG emission results of the catalyst produced using the U.S. average grid mix (baseline) were compared with those using three cleaner electricity sources: California (CA) grid mix, nuclear power, and wind energy. Details on the characteristics of each electricity source, including their respective GHG emissions, are provided in Table S9 of the ESI.†

Results and discussion

Techno-economic analysis

The net production cost of Pt/STO was estimated at $842 per kg for 1 wt% Pt loading. Fig. 3(a) displays the input of the breakdown of the different cost components on the catalyst cost. The analysis showed that the cost of raw materials is the largest contributor to the catalyst cost, especially the catalyst precursor (trimethyl(methylcyclopentadienyl)platinum(IV)). The incorporated SCV (i.e., the credits for recovering Pt metal) of $290 per kg has a significant role in reducing the net production cost. Details of the cost distributions to estimate the catalyst cost are provided in Table S10 of ESI.†

Approximately 76% of the total operational costs have been attributed to raw materials, mostly from the Pt precursor. However, the process utilities contribute to only 0.3% of the total operational cost, as illustrated in Fig. 3(b). The analysis also shows that the total capital investment has a minimum contribution to the net catalyst cost. Fig. 3(c) indicates that 86% of the total capital investment is attributed to the fixed capital investment, which includes direct and indirect capital investments, while the working capital contributed 14% of the total capital. No comparison of the catalyst Pt/STO production cost can be made with the industrial database since to the best of our knowledge, the catalyst has not yet been developed commercially. However, a cost comparison was conducted on the catalyst cost for the different Pt loading percentages on the various supports.[9,18]
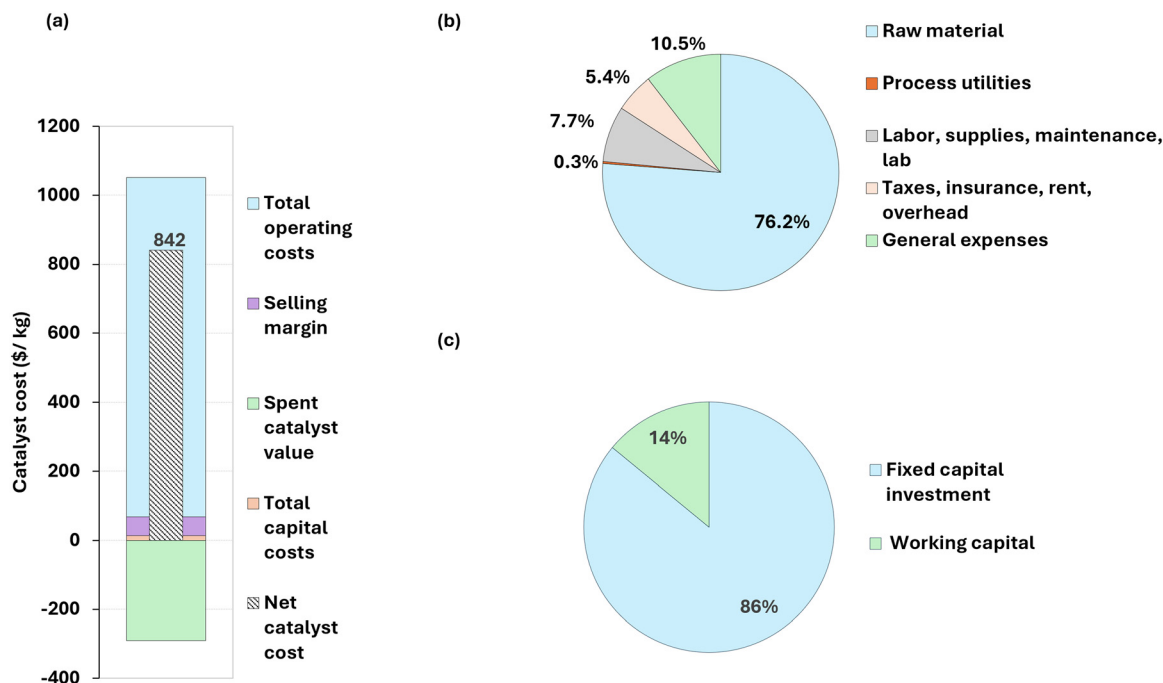
This journal is © The Royal Society of Chemistry 2025

Catal. Sci. Technol., 2025, 15, 4419–4429 | 4423

Fig. 3 Distribution of (a) the total overheads for the catalyst cost assessment, (b) the total operating costs for the calculated catalyst cost, and (c) the total capital costs for the evaluated catalyst cost.

The study reveals that the Pt loading percentage has a significant effect on the catalyst cost, as depicted in Fig. 4. In all studies, the catalyst cost is directly proportional to the weight percentage of Pt loading. This study revealed that the Pt/STO catalyst costs were \$598 and \$842 per kg catalyst for Pt loading rates of 0.5 and 1 wt%, respectively. Similarly, Van Allsburg $et\ al.$[9] observed purchase costs of the Pt/TiO$_2$ catalyst of \$153 and \$533 per kg catalyst with 0.5 and 2 wt% Pt loading, respectively. Additionally, Cappello $et\ al.$[18] reported the cost of the Pt/γ-Al$_2$O$_3$ catalyst at \$834 and \$3470 per kg

catalyst for loading rates of 2 and 10 wt%, respectively. An analysis exploring the recovery of ethanol, pentane, toluene, and dodecane, with recycling rates of 25, 50, and 75%, showed that the catalyst cost decreases by 2, 5 and 7% from the baseline cost (\$842 per kg), respectively. Detailed results are shown in Table S11 in the ESI.† This analysis did not consider the variation of equipment cost with the recovery rate. Note that an increase or decrease in the equipment expenses will change the catalyst cost associated with the solvent recycling.

A sensitivity analysis was performed on the Pt precursor cost, CapEX, OpEX, SCV, selling margin, plant size, total raw material cost, labor cost, and plant life to identify their impact on the net catalyst cost (Fig. 5). Among the selected parameters, the Pt precursor cost, OpEX, total raw material cost, and SCV had a profound effect on the synthesized catalyst cost. The total operating cost had the highest effect on the Pt/STO cost. A 50% reduction in the OpEX from the baseline case resulted in a 62% decrease in the catalyst cost from the baseline case. This points out that the catalyst cost can be reduced significantly by lowering the total operating cost of the synthesis procedure.

Another parameter with a significant impact on the catalyst cost is the Pt precursor cost. A 50% reduction in precursor cost leads to a 49% decrease in catalyst cost from the baseline case, while a 50% increase in Pt precursor cost leads to a 49% increase in the catalyst cost from the baseline. Likewise, for a 50% reduction in the total raw material cost, there is a 48% decrease in the catalyst cost compared to the baseline case, which confirmed that raw material costs had a profound effect on the catalyst production cost. This analysis also highlights
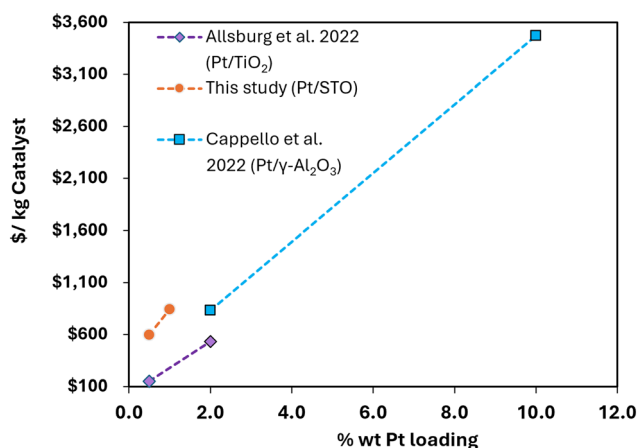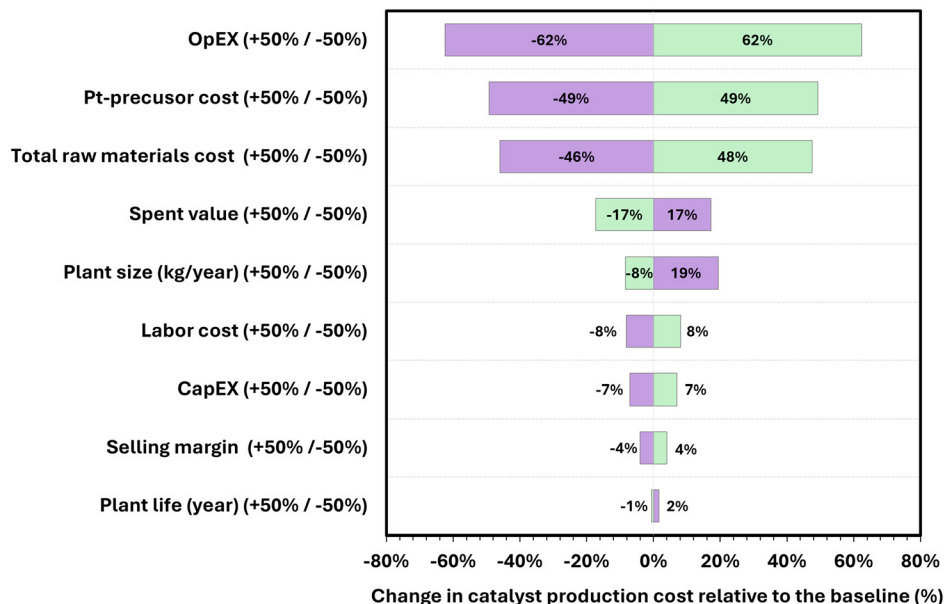

Fig. 4 The catalyst cost depends on the percentage weight of Pt loading in all studies. This study shows the cost of catalyst Pt/STO for 0.5 to 1 wt% Pt loading. Van Allsburg $et\ al.$ showed the Pt/TiO$_2$ catalyst purchase cost for 0.5 to 2 wt% Pt loading and Cappello $et\ al.$ presented the Pt/γ-Al$_2$O$_3$ catalyst purchase cost for 2 to 10 wt% Pt loading.

Fig. 5 Sensitivity analyses for the synthesis catalyst production cost. The production cost variation is due to the variation of different factors. Baseline catalyst cost = \$842 per kg catalyst. The dark green color and the lavender color represent the high value and the low value, respectively.

that the catalyst production cost could be decreased further by finding the raw materials, mainly the Pt precursor, at a lower cost. The other process inputs that affect the production cost of Pt/STO are the plant size and the SCV. With a 50% increase in the SCV and the plant size, the catalyst cost drops to 17%

and 8% from the baseline, respectively. When there is a 50% decrease in the SCV and plant size, the catalyst cost increases by 17% and 19% from the baseline, respectively. The findings show that the labor cost and CapEx also have a slight effect on the production cost.
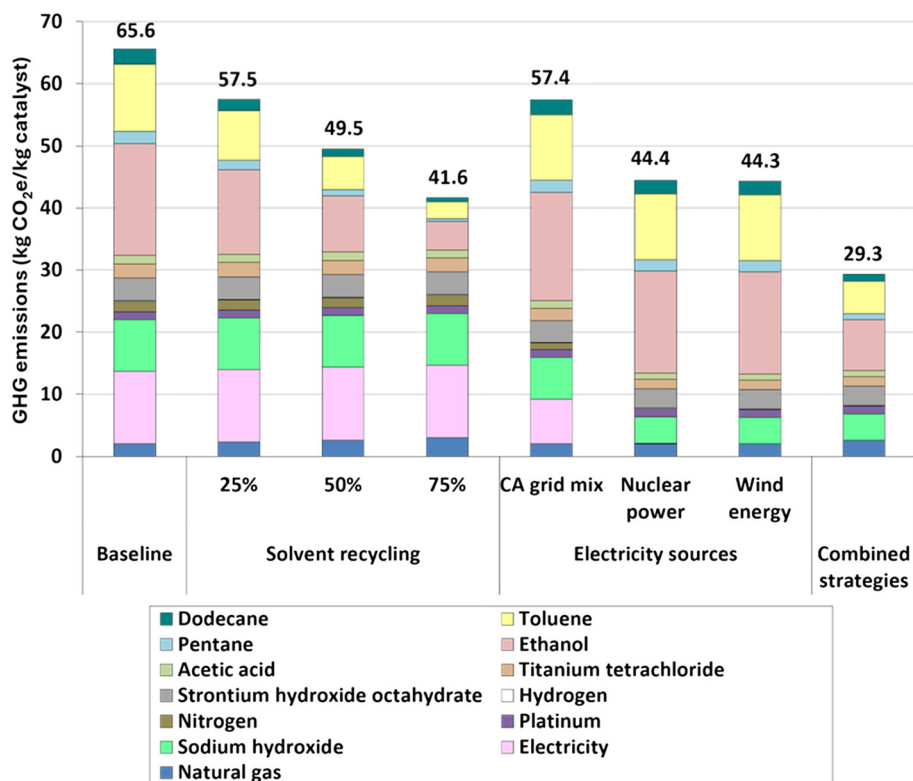
Fig. 6 GHG emissions of the baseline catalyst production and with the application of the different sensitivity analyses. The combined strategies evaluate the implementation of 50% material recycling and the use of wind energy. Tabulated results are presented in Table S12 of the ESI.†

This journal is © The Royal Society of Chemistry 2025

Catal. Sci. Technol., 2025, **15**, 4419–4429 | **4425**

Life-cycle analysis

Fig. 6 shows the estimated GHG emissions for the synthesis of the Pt/STO catalyst. The GHG emissions for this catalyst are estimated at 65.6 kg CO_2e per kg. The primary contributors to these emissions are the use of chemicals such as ethanol, toluene, and sodium hydroxide as well as electricity, which contribute 28, 16, 13, and 18% to the total GHG emissions, respectively. The significant consumption of chemicals is due to two main factors: the large volume of solvents required for reaction and washing processes, and the lack of solvent recovery in the current practice. Electricity is another driver of the emissions because of the high energy demand for ozone production, which is necessary in one of the treatment stages.

The GHG emissions of Pt/STO have been compared to those of other hydrogenolysis catalysts. Noble metals commonly employed in hydrogenolysis include ruthenium and palladium, which are added to different supports to synthesize different catalysts, such as Ru/C, Ru/CeO$_2$, Ru/TiO$_2$, Ru/Nb$_2$O$_5$, Ru/SrTiO$_3$, and Pd/C.[39–45] Also, alternative Pt catalysts like Pt/C are viable options. In the non-noble metal category, catalysts based on nickel, cobalt, copper, zinc, manganese, and iron are utilized. Some examples include Ni/SiO$_2$, Ni/ZrO$_2$, Ni/Al$_2$O$_3$, Ni/CeO$_2$, Ni/TiO$_2$, Co/TiO$_2$, Cu–Na/SiO$_2$, ZnO, and manganese and iron pincer complexes.[39,40,42–44,46] Research on the GHG emissions of these catalysts is limited; therefore, comparisons have been made using representative compounds from both noble and non-noble metal catalysts for which data are available.

The GHG emissions of Pt/STO are comparable to those of other noble metal catalysts such as Pt/C (55.1 kg CO_2e per kg) and Ru/C (80.4 kg CO_2e per kg).[47,48] However, these emissions may vary depending on the allocation method used or the type of support material. For instance, Pt/γ-Al$_2$O$_3$ has an estimated GHG emission of 6.9 kg CO_2e per kg, and Ru/C GHG emission can be reduced to 13.7 kg CO_2e per kg when mass allocation is used in the analysis.[30,48] Interestingly, although the energy consumption of some of these catalysts (Pt/C and Ru/C) is higher compared to Pt/STO, the extensive use of chemicals in Pt/STO results in similar GHG emissions.

Compared to non-noble metal catalysts, the GHG emissions of Pt/STO are significantly higher, ranging from approximately three times higher than those of Co/TiO$_2$ (17.1 kg CO_2e per kg) to as much as twelve times higher than Ni/Al$_2$O$_3$ (5.5 kg CO_2e per kg).[30,49] This indicates the importance of implementing strategies that minimize the use of chemicals, such as solvent recycling, and reduce the impact of electricity by using cleaner electricity sources.

The implementation of solvent recycling and the use of cleaner electricity sources resulted in significant GHG emission reduction for the catalyst production process (see Fig. 6). Based on the applied heuristic rule, solvent recycling may achieve GHG emission reductions of 12, 24, and 37% for 25, 50, and 75% recycling rates, respectively, compared to the baseline with no solvent recovery. Notably, despite an increase in energy consumption due to the separation through conventional distillation of ethanol, the increase in natural gas GHG emissions may be offset by the reduction in GHG emissions resulting from a decrease in the use of fresh solvents. A key recommendation for future research concerning this sensitivity analysis is to employ distillation design equations to achieve a more precise and robust estimation of the energy requirements for the ethanol separation process.

Alternative technologies, such as dividing wall columns, adsorption, and ultrasound separation, along with strategies like the implementation of heat pumping can reduce energy consumption and, consequently, the GHG emissions associated with solvent recovery processes. For instance, dividing wall columns could reduce the energy use by 30%, while adsorption could achieve 75% energy savings compared to conventional distillation.[38,50] Ultrasound separation could lower the GHG emissions of the separation process by 40% and the incorporation of heat pumping in the distillation process could lead to a 70% reduction in energy use compared to the conventional distillation process.[38,51]

Regarding the use of cleaner electricity sources, GHG emissions were reduced by 12, 32, and 32% when employing the CA electricity mix, nuclear power, and wind energy, respectively, compared to the baseline. Additionally, the simultaneous implementation of solvent recycling at 50% and the use of wind energy lowered the GHG emissions of catalyst production to 29.3 kg CO_2e per kg, representing a 55% reduction compared to the baseline.

Conclusion

This study conducted thorough TEA and LCA of the synthesis of Pt/STO catalysts used in hydrogenolysis for the upcycling of post-consumer plastics for commercial-scale production. To the author's knowledge, this is the first study to include the cost analysis and GHG emissions associated with producing a Pt/STO catalyst. The estimated cost of Pt/STO for 1 wt% Pt loading is $842 per kg. The TEA reveals that the cost of the raw materials is the dominant factor for the high cost of the catalyst; predominantly, the cost of the Pt precursor, trimethyl(methylcyclopentadienyl)platinum(IV). The sensitivity analysis indicates that the OpEX, Pt precursor cost, and SCV have a substantial influence on the cost of the synthesized catalyst. Furthermore, the outcomes of the sensitivity analyses highlight the significance for future researchers to focus on reducing the OpEx and Pt precursor cost in the overall synthesis process. The LCA indicates that the GHG emission of the catalyst is 66 kg CO_2e per kg, which is higher compared to other Pt-based catalysts. This is primarily due to the significant use of solvents and electricity, as well as the lack of recycling in the current production. However, simultaneous implementation of strategies such as 50% solvent recycling and the use of cleaner electricity sources, like wind energy, could reduce the GHG emissions from catalyst production by 56%, compared to the baseline production. Finally, this study offers important insights for researchers involved in the development of the type of catalyst described here by

4426 | *Catal. Sci. Technol.*, 2025, **15**, 4419–4429

This journal is © The Royal Society of Chemistry 2025

establishing key impact factors affecting the economic and environmental indicators of the process. The study also proposes guidance on strategies that can enhance cost-efficiency and reduce the environmental impact.

Notes

The submitted manuscript was created by UChicago Argonne, LLC, Operator of Argonne National Laboratory ("Argonne"). Argonne is a U.S. Department of Energy Office of Science laboratory under contract no. DE-AC02-06CH11357. The U.S. Government retains for itself, and others acting on its behalf, a paid-up nonexclusive, irrevocable worldwide license in said article to reproduce, prepare derivative works, distribute copies to the public, and perform publicly and display publicly, by or on behalf of the Government. The Department of Energy will provide public access to these results of federally sponsored research in accordance with the DOE Public Access Plan https://energy.gov/downloads/doe-public-access-plan.

The views and opinions of the authors expressed herein do not necessarily state or reflect those of the United States Government or any agency thereof. Neither the United States Government nor any agency thereof, nor any of their employees, makes any warranty, expressed or implied, or assumes any legal liability or responsibility for the accuracy, completeness, or usefulness of any information, apparatus, product, or process disclosed, or represents that its use would not infringe privately owned rights.

Nomenclature

ANL	Argonne National Laboratory
ALD	Atomic layer deposition
CA	California
CO_2	Carbon dioxide
GHG	Greenhouse gas
CapEx	Total capital costs
GREET	Greenhouse Gases, Regulated Emissions, and Energy Use in Technologies
LCA	Life cycle analysis
LCI	Life cycle inventory
MJ	Megajoule
MT	Metric ton
OpEx	The total operational costs
Pt/Al_2O_3	Platinum on alumina
$Pt/SiO_2–Al_2O_3$	Platinum on silicon dioxide and aluminum oxide
TEA	Techno-economic analysis
$Pt/SrTiO_3$	Platinum on strontium titanate
SOMC	Surface organometallic chemistry
sccm	Standard cubic centimeters per minute
SCV	Spent catalyst value

Data availability

The data supporting this article have been included as part of the ESI.† Please see the attached ESI.†

Conflicts of interest

The authors declare no competing financial interest.

Acknowledgements

References

1 G. Celik, R. M. Kennedy, R. A. Hackler, M. Ferrandon, A. Tennakoon, S. Patnaik, A. M. LaPointe, S. C. Ammal, A. Heyden, F. A. Perras, M. Pruski, S. L. Scott, K. R. Poeppelmeier, A. D. Sadow and M. Delferro, *ACS Cent. Sci.*, 2019, **5**, 1795–1803.

2 I. L. Peczak, R. M. Kennedy, R. A. Hackler, R. Wang, Y. Shin, M. Delferro and K. R. Poeppelmeier, *ACS Appl. Mater. Interfaces*, 2021, **13**, 58691–58700.

3 K. E. McCullough, I. L. Peczak, R. M. Kennedy, Y.-Y. Wang, J. Lin, X. Wu, A. L. Paterson, F. A. Perras, J. Hall, A. J. Kropf, R. A. Hackler, Y. Shin, J. Niklas, O. G. Poluektov, J. Wen, W. Huang, A. D. Sadow, K. R. Poeppelmeier, M. Delferro and M. S. Ferrandon, *J. Mater. Chem. A*, 2023, **11**, 1216–1231.

4 R. J. Witzke, A. Chapovetsky, M. P. Conley, D. M. Kaphan and M. Delferro, *ACS Catal.*, 2020, **10**, 11822–11840.

5 J. V. Lamb, Y.-H. Lee, J. Sun, C. Byron, R. Uppuluri, R. M. Kennedy, C. Meng, R. K. Behera, Y.-Y. Wang, L. Qi, A. D. Sadow, W. Huang, M. S. Ferrandon, S. L. Scott, K. R. Poeppelmeier, M. M. Abu-Omar and M. Delferro, *ACS Appl. Mater. Interfaces*, 2024, **16**, 11361–11376.

6 Y. Chen, A. Das, I. D. Duplessis, D. T. Keane and M. J. Bedzyk, *ACS Appl. Mater. Interfaces*, 2024, **16**, 26862–26869.

7 R. G. Carr and G. A. Somorjai, *Nature*, 1981, **290**, 576–577.

8 F. G. Baddour, L. Snowden-Swan, J. D. Super and K. M. Van Allsburg, *Org. Process Res. Dev.*, 2018, **22**, 1599–1605.

9 K. M. Van Allsburg, E. C. D. Tan, J. D. Super, J. A. Schaidle and F. G. Baddour, *Nat. Catal.*, 2022, **5**, 342–353.

10 P. T. Benavides, D. C. Cronauer, F. Adom, Z. Wang and J. B. Dunn, *Sustainable Mater. Technol.*, 2017, **11**, 53–59.

This journal is © The Royal Society of Chemistry 2025

Catal. Sci. Technol., 2025, **15**, 4419–4429 | **4427**

11 A. Dutta, M. Talmadge, J. Hensley, M. Worley, D. Dudgeon, D. Barton, P. Groenendijk, D. Ferrari, B. Stears, E. M. Searcy, C. T. Wright and J. R. Hess, *Process Design and Economics for Conversion of Lignocellulosic Biomass to Ethanol: Thermochemical Pathway by Indirect Gasification and Mixed Alcohol Synthesis*, NREL/TP-5100-51400, National Renewable Energy Lab, (NREL), Golden, CO, 2011.

12 E. C. D. Tan, M. Talmadge, A. Dutta, J. Hensley, J. Schaidle, M. Biddy, D. Humbird, L. J. Snowden-Swan, J. Ross, D. Sexton, R. Yap and J. Lukas, *Process Design and Economics for the Conversion of Lignocellulosic Biomass to Hydrocarbons via Indirect Liquefaction. Thermochemical Research Pathway to High-Octane Gasoline Blendstock Through Methanol/Dimethyl Ether Intermediates*, NREL/TP-5100-62402, National Renewable Energy Lab. (NREL), Golden, CO, 2015.

13 A. Dutta, J. A. Schaidle, D. Humbird, F. G. Baddour and A. Sahir, *Top. Catal.*, 2016, **59**, 2–18.

14 A. Dutta, A. Sahir, E. Tan, D. Humbird, L. J. Snowden-Swan, P. Meyer, J. Ross, D. Sexton, R. Yap and J. L. Lukas, *Process Design and Economics for the Conversion of Lignocellulosic Biomass to Hydrocarbon Fuels. Thermochemical Research Pathways with In Situ and Ex Situ Upgrading of Fast Pyrolysis Vapors*, NREL/TP-5100-62455, National Renewable Energy Lab. (NREL), Golden, CO, 2015.

15 S. Jones, P. Meyer, L. Snowden-Swan, A. Padmaperuma, E. Tan, A. Dutta, J. Jacobson and K. Cafferty, *Process Design and Economics for the Conversion of Lignocellulosic Biomass to Hydrocarbon Fuels: Fast Pyrolysis and Hydrotreating Bio-oil Pathway*, PNNL-23053, NREL/TP-5100-61178, PNNL: Richland, WA and NREL, Golden, CO, 2013.

16 G. Yadav, A. Singh, A. Dutta, T. Uekert, J. S. DesVeaux, S. R. Nicholson, E. C. D. Tan, C. Mukarakate, J. A. Schaidle, C. J. Wrasman, A. C. Carpenter, R. M. Baldwin, Y. Román-Leshkov and G. T. Beckham, *Energy Environ. Sci.*, 2023, **16**, 3638–3653.

17 International Energy Agency, International Council of Chemical Associations and Deutsche Gesellschaft für chemisches Apparatewesen, *Technology Roadmap: Energy and GHG Reductions in the Chemical Industry via Catalytic Processes*, Paris, France, 2013.

18 V. Cappello, P. Sun, G. Zang, S. Kumar, R. Hackler, H. E. Delgado, A. Elgowainy, M. Delferro and T. Krause, *Green Chem.*, 2022, **24**, 6306–6318.

19 A. D. Sadow, *Presented in part at the 2023 DOE Bioenergy Technologies Office (BETO) Project Peer Review*, Denver, CO, April, 2023.

20 G. Majeau-Bettez, T. R. Hawkins and A. H. Strømman, *Environ. Sci. Technol.*, 2011, **45**, 4548–4554.

21 K. Kingsbury and P. T. Benavides, *Life Cycle Inventories for Palladium on Niobium Phosphate (Pd/NbOPO4) and Zirconium Oxide (ZrO2) Catalysts*, ANL/ESD-21/6, Argonne National Lab. (ANL), Argonne, IL (United States), 2021.

22 GEA, GEA "Plug & Win" Triple win centrifuge skids for craft brewers, https://stiener.es/wp-content/uploads/2019/01/Centr%C3%ADfugas-GEA-Cerveza.pdf, (accessed May 30, 2024).

23 J. Tschernitz, in *Dry Kiln Operator's Manual*, ed. W. T. Simpson, 1991, pp. 239–256.

24 Cascade TEK, Vaccum Oven TVO-2, https://www.cascadetek.com/wp-content/uploads/2018/09/0740582-TVO-2-Spec-Sheet-1-3.pdf, (accessed May 30, 2024).

25 Agilent, Agilent IDP-7 Dry Scroll Vacuum Pump, Data Sheet, https://cdn.digivac.com/wp-content/uploads/2020/07/Agilent-IDP-7-Data-Sheet.pdf, (accessed May 30, 2024).

26 Anonymous vendor, Ozone generator, Personal communication, 2023.

27 ChemCatBio, CatCost v1.1.0, https://catcost.chemcatbio.org, 2021.

28 Federal Reserve Bank of St. Louis, Producer Price index by Commodity: Chemicals and Allied Products: Industrial Chemicals, https://fred.stlouisfed.org/series/WPU061, (accessed May 30, 2024).

29 Access Intelligence, LLC, Chemical Engineering Plant Cost Index (CEPCI), https://www.chemengonline.com/pci, (accessed April 30, 2024).

30 Argonne National Laboratory, Greenhouse gases, Regulated Emissions, and Energy use in Technologies Model® (2023 Excel), DOI: 10.11578/GREET-Excel-2023/dc.20230907.1, 2023.

31 P. R. Shukla and R. Slade, *Contribution of Working Group III to the Sixth Assessment Report of the Intergovernmental Panel on Climate Change. Climate Change 2022: Mitigation of Climate Change*, University Press, 2022.

32 S. H. Farjana, N. Huda, M. A. P. Mahmud and C. Lang, *J. Cleaner Prod.*, 2018, **196**, 1016–1025.

33 P. Caramazana-González, P. W. Dunne, M. Gimeno-Fabra, M. Zilka, M. Ticha, B. Stieberova, F. Freiberg, J. McKechnie and E. H. Lester, *Green Chem.*, 2017, **19**, 1536–1547.

34 P. Nuss and M. J. Eckelman, *PLoS One*, 2014, **9**, e101298.

35 S. G. Hibbins, Strontium and Strontium Compounds, *Kirk-Othmer Encyclopedia of Chemical Technology*, 2000.

36 M. Tsang, G. Philippot, C. Aymonier and G. Sonnemann, *Green Chem.*, 2016, **18**, 4924–4933.

37 European Solvents Industry Group, *Eco-profile of Three Hydrocarbon Solvent Groups: Cat. 3 solvents, Cat. 6 solvents, Cat. 8 solvents*, 2021.

38 A. A. Kiss and R. Smith, *Energy*, 2020, **203**, 117788.

39 L. Gan, Z. Dong, H. Xu, H. Lv, G. Liu, F. Zhang and Z. Huang, *CCS Chem.*, 2023, **6**, 313–333.

40 Z. Zhao, Z. Li, X. Zhang, T. Li, Y. Li, X. Chen and K. Wang, *Environ. Pollut.*, 2022, **313**, 120154.

41 J. E. Rorrer, C. Troyano-Valls, G. T. Beckham and Y. Román-Leshkov, *ACS Sustainable Chem. Eng.*, 2021, **9**, 11661–11666.

42 S. Sun and W. Huang, *JACS Au*, 2024, **4**, 2081–2098.

43 H. Wang and S. C. E. Tsang, *Cell Rep. Phys. Sci.*, 2024, **5**, 102075.

44 Y. Yuan, Z. Xie, K. K. Turaczy, S. Hwang, J. Zhou and J. G. Chen, *Chem Bio Eng.*, 2024, **1**, 67–75.

45 P. A. Kots, S. Liu, B. C. Vance, C. Wang, J. D. Sheehan and D. G. Vlachos, *ACS Catal.*, 2021, **11**, 8104–8115.

46 H. Mitta, L. Li, M. Havaei, D. Parida, E. Feghali, K. Elst, A. Aerts, K. Vanbroekhoven and K. M. Van Geem, *Green Chem.*, 2024, **27**, 10–40.

4428 | *Catal. Sci. Technol.*, 2025, **15**, 4419–4429

This journal is © The Royal Society of Chemistry 2025

47 S. Evangelisti, C. Tagliaferri, D. Brett and P. Lettieri, in *Modern Developments in Catalyst*, ed. G. Hutchings, M. Davidson, R. Catlow, C. Hardacre, N. Turner and P. Collier, World Scientific Publishing Europe Ltd., London, UK, 2017, pp. 289–312.

48 L. J. Snowden-Swan, K. A. Spies, G. J. Lee and Y. Zhu, *Biomass Bioenergy*, 2016, **86**, 136–145.

49 R. Aromaa-Stubb, M. Rinne and M. Lundström, *J. Sustain. Metall.*, 2024, **10**, 1795–1806.

50 S. Saini, A. K. Chandel and K. K. Sharma, *J. Cleaner Prod.*, 2020, **268**, 122357.

51 J. W. Ha, J. Liu, H. Feng, N. V. Sahinidis, H. Seo, J. J. Siirola and J. Na, *Cell Rep. Phys. Sci.*, 2024, **5**, 101785.

This journal is © The Royal Society of Chemistry 2025

Catal. Sci. Technol., 2025, **15**, 4419–4429 | **4429**